Influence of hole correlation on polarized-x-ray-emission spectra of single-crystal $YBa_2Cu_3O_{7-\delta}$

F. Werfel and G. Dräger
Fachbereich Physik der Martin-Luther-Universität, Halle-4010, Germany

J. A. Leiro
Department of Applied Physics, University of Turku, SF-20520 Turku, Finland

K. Fischer
Physical-Technical Institute, 6900 Jena, Germany

(Received 9 July 1991)

Polarized-x-ray O$K\alpha$ and Cu$L\alpha$ spectra of the high-T_c superconducting $YBa_2Cu_3O_{7-\delta}$ compound are presented. They show strong anisotropic features. The possible location of the holes, which are thought to be responsible for the superconducting properties, are discussed in the light of these experimental spectra. It seems that the CuO_2 and BaO planes are important layers for these oxygenlike holes. Because of charge transfer and correlation effects, characteristic spectral features are obtained.

I. INTRODUCTION

Core-line and valence-electron spectroscopies provide detailed information about the electronic structure of the Cu-based high-T_c superconductors. The recent results in this field clearly show strong on-site d-d and p-p Coulomb interactions to a large extent. Typically, x-ray photoemission spectroscopy, (XPS) core spectra of $YBa_2Cu_3O_{7-\delta}$(1:2:3) are characterized in the Cu $2p$ region by strong satellites[1,2] and features in the valence band at 9.5 and 12 eV are still discussed.[3,4]

In our recent investigation of the valence-electron spectrum of 1:2:3 by means of a combination of XPS, ultraviolet photoemission spectroscopy (UPS), and x-ray emission (XES), we determined the symmetry of the occupied states and tried to understand the observed differences between high-energy spectroscopic results and one-electron theory.[5] We estimated "local partial correlation shifts" of the theoretical Fermi level in the range 0.6–1.6 eV by comparing XES and calculations. The central phenomenon we have to understand is the response of the (correlated) valence electrons to a sudden creation of a core hole (as a long-standing problem in high-energy spectroscopy). The inherently acting parameters, e.g., the intrasite and intersite Coulomb repulsion energy U and the charge-transfer energy Δ relative to the bandwidths, have been adapted successfully in the last decade in order to explain core-hole spectra of transition-metal compounds.[6,7]

A similar extended Hubbard model to describe the basic valence-band (VB) electronic structure of high-temperature superconductors (HTSC's) is recently proposed by Ramaker, Turner, and Hutson[8] and Fujimori, Takayama-Muromachi, and Uchida[9] in terms of a Cu $O_n^{(2n-2)}$ cluster. The correlation parameters of interest are given to $U_d=9.5$ eV, $U_p=12$ eV, and $U_{pp0}=4.5$ eV for 1:2:3 material which include, especially, the intersite repulsion energies $U_{dp}\approx 1$ eV and U_{pp0} (i.e., between neighboring Cu-O and O-O atoms, respectively). The importance of the oxygen contribution to correlation phenomena seems evident because, according to experimental results, the carriers in most of the HTSC's are holes created and localized primarily on oxygen atoms. The calculations of the oxygen-related U parameters are still hampered by the situation that the basic Wannier functions of the bandlike O $2p$ states are not well defined compared to nearly localized Cu $3d$ orbitals. Therefore, O site and symmetry-selective experiments are of substantial interest providing an independent measure and proof of these parameters.

In the present contribution, we provide spectral information on the symmetry of the occupied O $2p$ and Cu $3d$ orbitals utilizing polarized-x-ray-emission spectroscopy (PXES) at single crystal $YBa_2Cu_3O_{7-\delta}$ for O $K\alpha$ and Cu $L\alpha$. The polarization is achieved with respect to the characteristic crystal geometry of 1:2:3, i.e., parallel and perpendicular to the (a,b) plane. In comparison with conventional XES, the method is capable of probing the occupied local partial density of states (DOS) at O and Cu sites separately with additional selectivity obtained by orienting the vector of polarization **e** (the electric vector of x rays) relative to the preferred crystal axis. The obtainable information of PXES are complementary to electron-energy-loss spectroscopy[10] (EELS) and polarized x-ray-absorption spectroscopy[11] (XAS) which probe the unoccupied DOS in different crystalline directions. Polarization-dependent experiments on oxygen sites are still performed rarely. Nücker *et al.*[10] proposed hole localization in the O $2p$ orbitals of the CuO_2 plane in 1:2:3 studying the O $1s$ transition into unoccupied $2p$ orbitals by EELS. Experimental facts favor the holes located in $p\sigma$ bonds, but a contribution from in-plane $p\pi$ orbitals cannot be excluded. Recently, Zaanen, Alouani, and Jepsen[12] reinterpreted the experimental results of Nücker *et al.* by using a band-structure calculation. They concluded that the peaks at the O K-absorption edge could be largely ascribed to the van Hove singularities in the chain bands. From XAS measurements, Bianconi *et al.*[13] concluded the appearance of holes largely in off-plane orbitals p_z in contrast with Nücker *et al.*[10] XPS

data interpretation of O-related structures are even more different. The O 1s main line appears at 528.8 eV. An O 1s feature at about 531.0 eV in 1:2:3 material could be sensitive to special conditions in the sample preparation process generating a well-ordered superstructure on O sites and giving rise to the additional component. In each case of analyzing experimental spectra, an understanding of the nature of the many-body problem in the particular system seems to be an ultimate requirement.

With respect to this, the here-presented x-ray-emission spectra have several advantages over XPS results which enter into the various core-hole–valence-electron interaction. In XPS, the different spectral main and satellite components are broadened by configuration interaction mixing and by the situation that many final-state multiplets can be attained rather than displaying specific multiplets. XES and, moreover, PXES are determined by $\Delta l = \pm 1$ and $\Delta m = -1, 0, 1$ for the orbital angular quantum number and the magnetic quantum number, respectively. Only a limited number of states are accessible. Furthermore, the XPS initial-state valence electrons experience the full potential of an unscreened core hole giving rise to strong satellites in the final state. Because the lifetime of the excited x-ray states exists, comparable longer orbital relaxation and screening before the core-hole decay will reduce the attainable final states in the x-ray process considerably.

Finally, we notice as an extrinsic advantage of XES that the technique is less surface sensitive and ambiguities due to surface contamination and alteration are avoided. The measurements were focused on high-purity $YBa_2Cu_3O_{7-\delta}$ single crystals and compared with previous integral spectra of superconducting 1:2:3 ceramic samples.

II. EXPERIMENT

A. Samples and instrumentation

The starting composition of single-crystal growth was $YO_{1.5}$ 6.5 mol%, $BaCO_3$, 22.5 mol%, and CuO 71.0 mol%. The $YBa_2Cu_3O_{7-\delta}$ compound is formed by a peritectic reaction. Typically, crystal plates grow into melt-depleted cavities thus allowing mechanical separation after finishing the growth experiment. In the as-grown state, the crystals do not show superconducting properties above 80 K. After annealing in oxygen atmosphere at 680 °C for 12 h, superconductivity was observed by the discontinuity of the magnetic susceptibility. $YBa_2Cu_3O_{7-\delta}$ ($\delta \sim 0.1$) single crystals with $T_c \sim 90$ K were selected with respect to well-shaped faces in order to allow an easier sample orientation. The lattice structure and crystal orientation with Laue pattern exhibit the preferential growing in $[a,b]$ direction resulting in plate-like small twinned crystals, as usual in the case of $YBa_2Cu_3O_{7-\delta}$ samples. The stoichiometry and phase purity was checked by electron probe microanalysis (EPMA) approaching the 1:2:3 ratio without indication of impurities. The estimation of the total oxygen concentration by EPMA is uncertain because of the lack of reliable ZAF correction parameters. The polarized-x-ray-emission spectra has been obtained on a dedicated long-wavelength spectrometer channel with a RAP monochromator ($2d = 26.118$ Å) of an electron probe microanalyzer [Applied Research Laboratories (ARL)]. The exciting primary beam was set to 5 kV, 200 nA at standard vacuum conditions ($\sim 10^{-3}$ Pa). In order to prevent or minimize possible sample degradation, the primary beam was slightly defocused to approximately 10-μm spot size.

The free-standing single crystals in the dimensions of about $2 \times 2 \times 0.5$ mm^3 were mounted on a special sample holder with the emitting surface parallel to the orthorhombic c axis and has been conducted to ground potential. The polarized spectra are registered for two special positions of the emitting sample relative to the polarization vector $\mathbf{e}$ of the preferentially reflected radiation. (Fig. 1, $c \| \mathbf{e}$ and $c \perp \mathbf{e}$). The partially polarized O $K\alpha$ ($2p \rightarrow 1s$) and Cu $L\alpha$ ($3d, 4s \rightarrow 2p$) x-ray-emission spectra have been accumulated in a computer-controlled step procedure at Bragg angles Θ of 64.5° and 30.7°, respectively. Both angles deviate from the ideal polarization case of $\Theta = 45°$ and, hence, a correction procedure has been performed (see subsequent part). It should be mentioned that the measured spectra of the two crystal orientations result from the identical spot position by turning the sample 90° around the primary beam directions as it is illustrated schematically in Fig. 1. Therefore, the observed spectral intensities are not obscured by self-absorption or by position-dependent composition alterations. No changes in the oxygen concentration before and after the x-ray measurement could be observed.

The measured peak positions of the polarized spectra were aligned with reference to the O $K\alpha$ emission of SiO_2 (quartz) at 526.0 eV and to Cu $L\alpha$ of metallic Cu at 930.1 eV.[14] At optimal Rowland circle adjustment, the energy resolution is approximately 0.4 and 0.7 eV for O $K\alpha$ and Cu $L\alpha$, respectively. Corresponding broadening due to the lifetime of the O 1s and Cu $2p_{3/2}$ core levels is 0.2 and 0.7 eV, respectively.[15,16]

B. Polarized-x-ray-emission valence-band spectra

In the dipole approximation the x-ray-emission intensity $I(\omega, \mathbf{e})$ emitted from a single crystal is determined by a transition from an initial core state $|\Psi_c\rangle$ to a final valence state $|\Psi_{kv}\rangle$ with the energies E_c and E_{kv}, respectively. The intensity

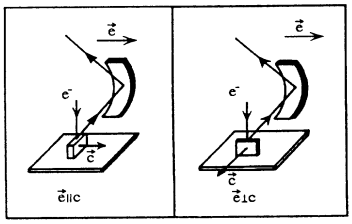

FIG. 1. Geometrical setup for measuring polarized-X-ray-emission spectra (PXES) of single crystals.

$$I(\omega,\mathbf{e})\sim\omega^3\sum_{k\nu}^{\text{occ}}|\langle\Psi_c|\mathbf{e}\cdot\mathbf{r}|\Psi_{k\nu}\rangle|^2\delta(E_{k\nu}-E_c-\hbar\omega) \quad (1)$$

depends on the orientation of the polarization vector **e** (parallel to the electric field component of the emitted radiation) with respect to the axis $\eta=x,y,z$ of a principle coordination system which is determined by the crystallographic axis of the sample. The $k\nu$ summation is over all occupied states.

The principal intensities $I_\eta(\omega)$ for a polarization parallel to the principal axis η can be measured by an appropriate experimental arrangement.[17] In practice, one accumulates the spectra predominantly polarized parallel and perpendicular to an estimated preferred crystallographic axis, e.g., in our case, the c axis of the orthorhombic 1:2:3 single crystal.

Because of the twinning in the (a,b) plane of the 1:2:3 crystals, the angular distribution of x-ray emission must be cylindrically symmetric relative to the c axis and is a function only of the polar angle ϑ between the polarization vector **e** and c. If we denote $I_x=I_y=I_\sigma$ and $I_z=I_\pi$, we obtain

$$I(\omega,e)=I_\sigma(\omega)\sin^2\vartheta+I_\pi(\omega)\cos^2\vartheta \quad (2)$$

and, in the case of an idealized polycrystalline sample,

$$I(\omega)=\tfrac{1}{3}(2I_\sigma+I_\pi)\ . \quad (3)$$

According to these geometrical considerations, and because $I_x=I_y=I_z$, no anisotropic intensity distribution is expected by investigating single crystals with cubic lattice symmetry. Polarized-x-ray-emission spectra display a selected part of the density of occupied states. More detailed formulas and calculated results (of hexagonal structures) are given in Ref. 18.

In practice, the geometrical conditions limit the directly separable I_η components due to deviations from the ideally linearly polarized case $\Theta=45°$, having, in most situations, a polarization $q=|\cos2\Theta|^2\neq0$ (for an ideally mosaic crystal monochromator). In addition, the takeoff angle α of the microprobe (52.5°) causes mixing effects between I_π and I_σ. Therefore, the spectra taken for a certain orientation, where radiation with $\mathbf{e}\perp c$ is preferentially registered, for example, always had contributions of $\mathbf{e}\parallel c$.

As a consequence, the measured spectra

$$\begin{aligned} I_\parallel^{\text{expt}}&=I_\pi+qI_\sigma\ ,\\ I_\perp^{\text{expt}}&=I_\sigma(1+q\cos^2\alpha)+I_\pi q\sin^2\alpha \end{aligned} \quad (4)$$

are a linear superposition of the pure intensities I_π and I_σ with coefficients depending on the special sample orientation. In order to obtain the true intensities, the coefficient matrix has to be inverted and multiplied with the measured and suitable normalized intensities $I_\parallel^{\text{expt}}$ and $I_\perp^{\text{expt}}$. In our case, we had a point-to-point transformation and uncertainties in the energy calibration would cause discontinuities and singularities in the calculated spectra. The O $K\alpha$ spectra have a typical statistical uncertainty of $\pm2.5\%$ and the Cu $L\alpha$ spectra of $\pm1.6\%$ estimated from the maximum intensity.

III. RESULTS

A. O $K\alpha$

Figure 2 shows the O $K\alpha$ emission of single crystal $YBa_2Cu_3O_{7-\delta}$ for the polarization vector **e** parallel and perpendicular to the orthorhombic c axis, denoted by $K(\parallel)$ and $K(\perp)$, respectively. The lines through the points were determined by using a simple three-point smoothing algorithm. The O $K\alpha$ emission probes the local occupied DOS with $2p$ symmetry at the O sites assuming the transition matrix element independent of energy in the considered region. The spectra of different polarizations are referenced and adjusted with respect to the well-known 532.0-eV satellite structure [attributed to an oxygen reflectivity anomaly in acid phtalat (AP) monochromators] assuming no polarization dependency of this feature.

Generally, a strong anisotropy is observed by comparing the two spectra in Fig. 2 obtained from different single-crystal orientations relative to the position of the polarization vector **e**. Between the two orientations, three main differences are obvious: (i) a peak shift of about 1 eV, (ii) an additional broad low-energy shoulder in the $K(\perp)$ spectrum separated 4.5 eV from the max-

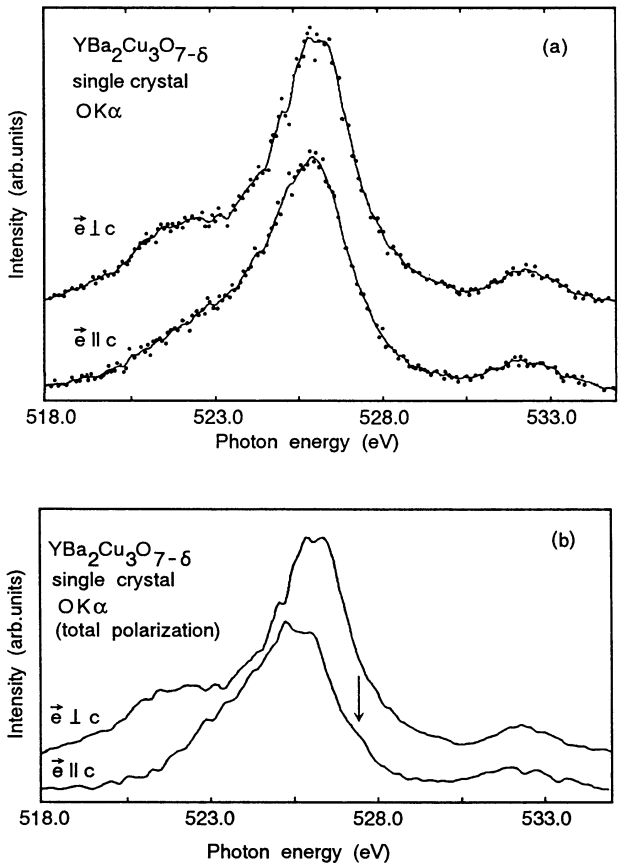

FIG. 2. Polarized O K single-crystal $YBa_2Cu_3O_{7-\delta}$ spectra perpendicular ($\perp$) and parallel ($\parallel$) to the orthorhombic c axis. (a) Original spectrum and (b) corrected for total polarization. The possible local triplets $^3B_1$ are shown by an arrow.

imum, and (iii) a less structured overall shape of the $K(\|)$ spectrum relative to the $K(\perp)$ orientation.

Further on, the p orbital anisotropy is documented in the different FWHM of 2.7 and 3.2 eV for $c\perp e$ and $c\|e$, respectively. Because of the O $2p\rightarrow 1s$ transition, principally O $1s$, BE shifts between the three different O sites in 1:2:3 could cause part of the observed anisotropy. We have performed systematically XPS O $1s$ measurements on 1:2:3 ceramic samples using monochromatized excitation obtaining O $1s$ symmetric lines at 528.8–529.0 eV (always with a well-separated smaller component at about 531.0 eV). Hence, we assume the O $1s$ threshold at 528.8 ± 0.2 eV as an averaged value of all oxygen sites.

The O $K\alpha$ peak shift between the two orientations $\|$ and $\perp$ as it is already observed in the original measurements and is visible more clearly in the corrected spectra of Fig. 2(b). The spectra correction for total polarization is performed by a mathematical procedure described in Sec. II [Eqs. (4)]. The total linearly polarized components $I_{\|}$ and $I_{\perp}$ confirm the strong anisotropic behavior. The above-indicated spectral differences between the parallel and perpendicular crystal orientation are more pronounced after correction owing to band shifts and fine structure. In O $K\alpha(\perp)$ at 522 eV, now a subband of substantial intensity is observed well separated 4.5 eV from the main peak. The $p_{x,y}$ states in $K(\perp)$ maximum appear at 1 eV higher energy relative to p_z orbital [$K(\|)$ spectrum]. It is interesting to note that, in the case of the O K-absorption spectra, the source of the energy shift has been observed (Nücker *et al.*). This effect has been explained by Zaanen *et al.* to be due to about 1 eV smaller binding energy of the O $1s$ core level of the O(4) atom compared with the corresponding binding energy of the chain O(1) and the in-plane O(2), O(3), $1s$ states. On the long-wavelength side of the O $K\alpha(\perp)$, smaller but reproducible structures at 524 and 525 eV appear while the corresponding O $K\alpha(\|)$ part between 522 and 525 eV is relatively flat. However, in the totally polarized spectrum, a weak shoulder at 527.0 eV ($\|$) on the high-energy side of the main peak probably indicates local triplets $^3B_1$.[19] In that case there would exist holes both in the BaO plane and in the CuO_2 plane having largely an oxygen character. This would possibly mean that the local singlets $^1A_1$ close to the Fermi level would have a larger binding energy than that of the local triplets $^3B_1$ for a 1:2:3 compound. It is also suggested by the results from configuration-interaction (CI) cluster calculations by Fujimori for a $(CuO_5)^8$ cluster which take into account ligand-to-metal transfer.[20]

In Fig. 3, we show a comparison of two O $K\alpha$ spectra. The lower one is measured previously on a $YBa_2Cu_3O_{7-\delta}$ ($\delta\sim0.1$) ceramic sample and is comparable with the corresponding results of other authors.[21] The upper spectrum is obtained by a mathematical synthesis according to $I=(2I_{\perp}+I_{\|})/3$ using the fully polarized components of Fig. 2(b). Evidently, the spectral similarities are remarkable, especially concerning the overall position and shape of the main band. The low-energy shoulder at 522 eV is observed in the ceramic spectrum, however, with comparable less intensity. The origin of the lower spectral weight in the ceramic spectrum compared with the sum of the polarized components could be a crystalline orientation effect or contributions from grain boundaries and intergrain species covering and smoothing characteristic spectral bulk features. Because of the good agreement of the two spectra in Fig. 3, we conclude that our polarization measurements and the correction procedure outlined with respect to the estimated individual O $K(\|)$ and O $K(\perp)$ components seem reasonable. If large single-phase, untwinned 1:2:3 crystals are available, a principle separation between the a and b axes related x-ray components becomes possible. Our approach to treat the plane lattice parameters as $a\approx b$ emphasizes small restrictions only.

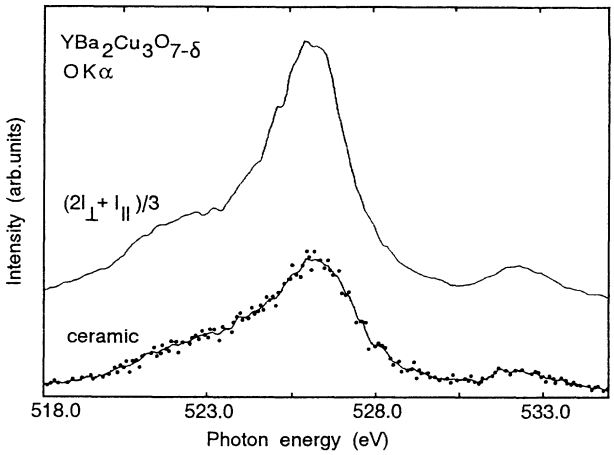

FIG. 3. O K spectrum of ceramic $YBa_2Cu_3O_{7-\delta}$ sample compared with summarized single-crystal polarization spectra according $I=(2I_{\perp}+I_{\|})/3$.

B. Cu $L\alpha$

The polarized measured and corrected Cu $L\alpha$ (Cu $3d$, $4s\rightarrow 2p_{3/2}$) spectra in Figs. 4(a) and 4(b), respectively, demonstrate the anisotropic properties of the occupied Cu $3d$ ($4s$ contributes less) orbitals in 1:2:3 material. Again, we measured the spectra from a single-crystal orientation in the two positions with respect to the polarization vector e.

We observe for the Cu $L\alpha$ spectra similar trends and behavior compared to the orientation results on O $K\alpha$. The peak maxima were located at 930.2 ± 0.2 eV ($\perp$) and 929.6 ± 0.2 eV ($\|$) and the FWHM estimated to 4.4 and 4.7 eV, respectively. The Cu $L\alpha$ spectra are more symmetric than the O $K\alpha$, but final decisions about this property depend strongly on the background. While the in-plane spectrum Cu $L(\perp)$ exhibits four characteristic structures and additional weaker features, the $L(\|)$ band shape is comparably structureless without clear spectral features on both sides of the peak maximum. In a first approach this situation would indicate the strong in-plane σ Cu(2)-O(2,3) $d_{x^2-y^2}$ bonds in Cu$L\alpha(\perp)$ and the presumably dominating Cu(1)-O(4) d_{z^2} bond along the c direction. The inherent energy scale of the here-

projected Cu d orbitals is determined by a combination of x-ray and XPS parameters.

From XPS measurements, we obtain a Cu $2p_{3/2}$ spectrum characterized by two principal structures at 933.5 eV and a broader less intense band between 940 and 945 eV representing typical final states of the configuration Cu $2\underline{p}3d^{10}\underline{L}$ and Cu $2\underline{p}3d^{9}$, respectively. The energy separation of approximately 9 eV is close to the energy of the core-hole–d-electron Coulomb attraction. The question arising from the XPS situation concerns the existence of only one x-ray-emission band. The energy-level scheme for the XES final states shows that, upon x-ray excitation because of relaxation and screening processes of the type $2\underline{p}3d^{9}\rightarrow 2\underline{p}3d^{10}\underline{L}$, mainly the $d^{10}\underline{L}$ state is the x-ray-active initial state for Cu $L\alpha$ leading to a $3d^{9}\underline{L}$ final state. Hence, the threshold energy for the $L\alpha$ spectra should be 933.3±0.2 eV. In a similar way, we determined from the O 1s spectrum the oxygen threshold energy to 528.8 eV.

Assuming the above-described threshold energies for the Cu $L\alpha$ and O $K\alpha$ transitions, a correlation of the polarized spectra on a common energy scale can be shown in Fig. 5. It is interesting to note that there might be a hybridization between the Cu 3d and O 2p bands as far as the broad feature at about 7 eV from the Fermi level is concerned. This is evident if one compares the Cu $L\alpha$ and O $K\alpha$ spectra in the case when e⊥c as can be seen from Fig. 5.

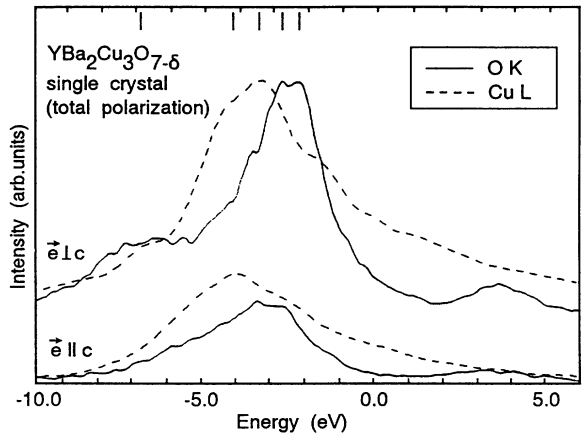

FIG. 5. Polarized O K and Cu L spectra combined in a common energy scale using the reference of O 1s and Cu $2p_{3/2}$ energies obtained by XPS.

Again, as a related proof of the relevance of the measured and corrected Cu $L\alpha$ polarized components we compare the composite spectrum $(2I\perp+2I\parallel)$ according to Sec. II with a previously measured Cu $L\alpha$ integrated result on a ceramic 1:2:3 sample in Fig. 6. A sufficient agreement between the two spectra can be established. A closer inspection of Fig. 6 confirms the already in O $K\alpha$ observed small differences between the spectra demonstrating the generally higher information content in polarized spectra relative to integral measurements. On the high-energy side of the Cu $L\alpha$ spectrum, the intensity is quite high if one compares with that of the low-energy side. There are some features extending above the assumed Fermi level energy position 933.3 eV as well.

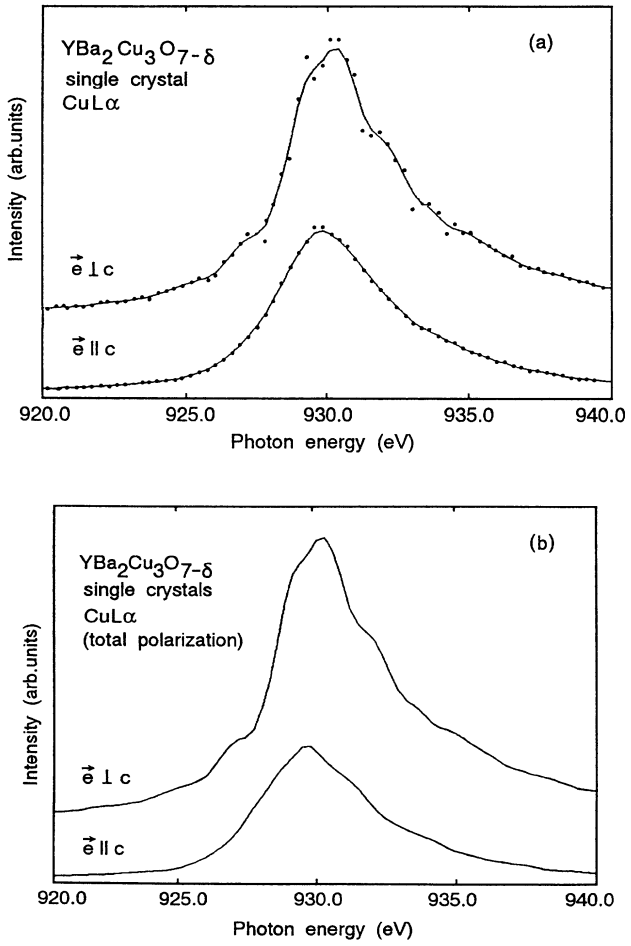

FIG. 4. The same as Fig. 2 but for Cu L spectra.

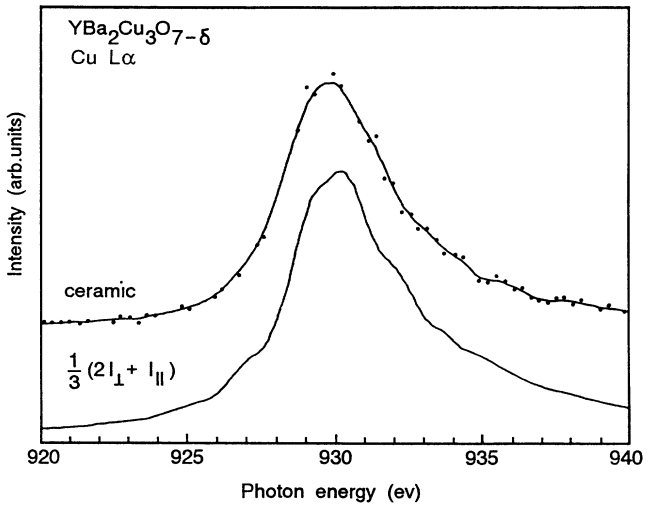

FIG. 6. The same comparison between spectra of single crystal and ceramic material as in Fig. 3 for Cu L.

These can be attributed to the high-energy satellites caused by Cu $3d$-like holes which are mainly due to the Coster-Kronig transition in the Cu atom.[22]

We notice in Cu $L\alpha(\perp)$ a fine structure at 926.0 eV, separated about 4 eV from the main peak. As in the case of O $K\alpha(\perp)$, this small subband arises from orbitals in the (a,b) plane providing experimental arguments for an essential geometrical localization of the involved electronic states. Following our XPS and UPS measurements on polycrystalline samples,[5] the 1:2:3 valence band in the occupied part extends to about 7 eV from the Fermi energy E_F in good agreement with energy range obtained by calculations.[23] Therefore, the observed x-ray structure located at about 7 eV relative to E_F can hardly be solely explained in terms of the initial DOS. It should also be mentioned that a corresponding satellite structure separated by a comparable energy from E_F or from principal core lines is neither observed in photoemission VB spectra nor in XPS core-level measurements. On the other hand, we have to remember the highly selective character of PXES transitions reducing considerably the number of accessible states on the same atom. Hence, we suggest that Coulombic interactions may contribute to the unusual subband in the polarized spectra by transitions to oxygen in-plane orbitals (hybridized with Cu d states) interacting with orbitals possessing holes on neighboring sites as well as to oxygens in the Cu-O chains. As shown in Fig. 7, we have measured polarized O $K\alpha$ spectra of single crystals with reduced oxygen concentration ($\delta \approx 0.4$) and compared with those of the $\delta \approx 0.1$ samples. Following structure analysis, oxygen release removes O(1) atoms from the Cu-O chains. With respect to the 522-eV shoulder in O $K\alpha(\perp)$, we observe (i) an energy shift of the shoulder towards the main peak and (ii) a more localized character of the shoulder. In addition, the O $K\alpha(\perp)$ main peak of $\delta \approx 0.4$ is shifted with respect to the $\delta \sim 0.1$ spectrum by about 0.5 eV to lower energy. Interestingly, this shift can be observed only for the case where polarization vector e is perpendicular to the c axis ($e \perp c$). This result emphasizes the role of the plane and/or the chain contributions.

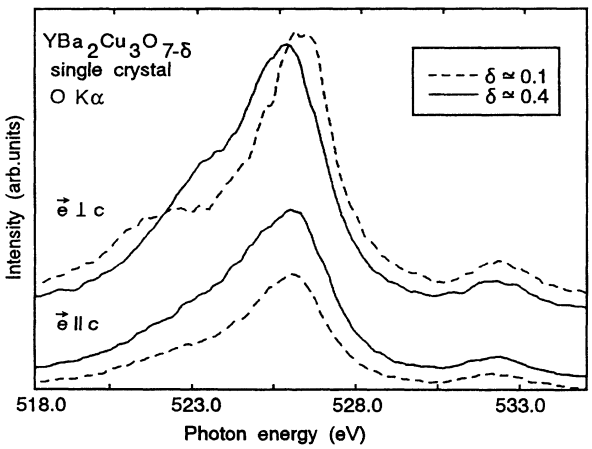

FIG. 7. O $K\alpha$ spectra, when the polarization vector e is polarized $\perp$ and $\parallel$ to the c axis, obtained from 1:2:3 single crystals of different oxygen concentrations ($\delta \approx 0.1$ and 0.4).

IV. INTERPRETATION AND DISCUSSION WITH RESPECT TO HOLE CORRELATION EFFECTS

Basically, our O $K\alpha$ and Cu $L\alpha$ polarized emission spectra display two effects with respect to the projected symmetry of orbitals under consideration. A strong anisotropic behavior is judged by comparing spectra of the *same atom* parallel and perpendicular to the (a,b) plane while, on the other hand, a consistent picture of the electronic and hole states can be terminated by analyzing spectra of different atoms but obtained on the *same direction.*

In order to interpret the polarized-x-ray-emission spectra properly, we refer to a theory of an extended Hubbard model based on a $CuO_n^{(2n-2)}$ cluster and reported recently.[8] The model describes the electronic structure when intrasite and intersite Coulomb repulsion energies are larger than the free-electron Fermi energy and dominate covalent or hybridization effects. This should not mean that hybridization is excluded completely. We would also like to point out that the cluster model seems to describe the essential phenomena, however, because of the inherent restrictions (limited number of atoms, neglected interaction with Y and Ba atoms) at least quantitative differences compared to experiments may appear.

In a geometrical consideration of Y-Ba-Cu-O, the basic elements are the CuO_3 ribbons along the b direction and the CuO_2 planes in the (a,b) direction. The principal orthorhombic lattice structure gives rise to the orientation-dependent physical properties. With respect to the existence of holes in the structure the CuO_n cluster model assumes that the hole is shared between the Cu $3d$ and O $2p$ valence orbitals in the ground state. Upon x-ray excitation, the additional core hole will influence the ground state leading to a double-hole initial-state configuration. In the case of a Cu-O cluster approach, the initial x-ray states have the same configuration as the XPS final states:[2] O $1\underline{s}$ Cu d^9 (528.8 eV) for O $K\alpha$ transitions and analogous Cu $2\underline{p}d^9$ (940–944 eV) and Cu $2\underline{p}d^{10}\underline{L}$ (933.3 eV) for the Cu $L\alpha$ spectrum. In the XPS mechanism, the x-ray core-hole excitation will induce screening and charge-transfer interactions of the type Cu $2\underline{p}d^9 \rightarrow$ Cu$2\underline{p}d^{10}\underline{L}$ on Cu sites. We believe the latter configuration is largely x-ray active. According to the inherent x-ray transition mechanism, the final states reached by O $K\alpha$ and Cu $L\alpha$ have identical configurations, i.e., O $1\underline{s}2p^6$ Cu $d^9 \rightarrow$ O $1s$ Cu $d^9\underline{L}$ and Cu $2\underline{p}d^{10}\underline{L} \rightarrow$ Cu $2\underline{p}d^9\underline{L}$, respectively. The final states are again two-hole states. The selective character of the x-ray process described above prevents the appearance of satellite structures as we observe in the corresponding XPS O $1s$ and Cu $2p$ spectra. Being aware of these mechanisms, we analyze the orientation-dependent x-ray spectra, particularly with respect to hole interactions in the 1:2:3 structure.

Earlier calculations based on final-state configuration interaction on a CuO_6 cluster and including interatomic Coulomb and exchange interactions between d electrons

exhibit a broad level structure around 2 eV relative to E_F.[24] Alternatively, initial-state p orbital splitting into bonding and antibonding components in the (a,b) plane may also be the origin. In view of the geometrical factors involved in the polarized spectra the O(1), O(2), and O(3) sites should contribute to the O $K\alpha(\perp)$ spectrum, principally. For $K\alpha(\parallel)$, mainly orbital contributions from O(4) are expected. Therefore, whether the observed $(\perp)$ and $(\parallel)$ structures are a projection of the O $p\sigma$ orbitals separated by about 0.5 eV from in-plane O p_π, we cannot finally decide. The main feature in the $L\alpha(\perp)$ spectrum is connected with the Cu $3d_{xy}$ symmetry which is associated with the π bonding of the Cu $3d$-O $2p$ coupling.

We concentrate now on the question of where in the structure of $YBa_2Cu_3O_{7-\delta}$ the holes are localized. The observed subband in O $K\alpha(\perp)$ separated about 7 eV from the threshold (Fermi level) could be explained[5] by transitions $cd \rightarrow pd$ (now in the hole picture; c denotes a core hole) and a simultaneous charge-transfer process $pd \rightarrow pp^0$, i.e., an orthoneighboring two-hole final state.[8] This two-hole final state can be reached directly by a $cp^0 \rightarrow pp^0$ transition where, in the initial state, the core hole c is in an orthoneighboring position with respect to a valence hole p^0. In this case the polarized-x-ray-emission spectra give experimental evidence and weight that these holes are largely localized in the plane especially for the $3d^{10}\underline{L}^2$ configuration. Beyond the model of Ramaker,[9] our polarized O $K\alpha(\perp)$ spectra of samples of different oxygen concentration in Fig. 7 evidently depend on the number of the O(1) atoms in the Cu-O chain. This behavior is also supported by other theoretical calculations.[12,24] A comparable orthoneighboring situation is given by the pair O(1)-O(4) in a plane parallel to the c axis. But, in this direction, the corresponding polarized O $K\alpha(\parallel)$ and Cu $L\alpha(\parallel)$ spectra do not show any spectral feature in the expected way from final-state pp^0 transitions. Furthermore, following the model of the two-hole final-state interactions, which are responsible for the observed subband, we observe the structure in *both* $(\perp)$ spectra at about the same energy from E_F. From this correspondence we suggest hole information in orbitals with predominantly O $p\sigma$ character.

Our suggestion is based on the assumption that the coupling in the σ band between d and p orbitals of the CuO_2 plane is considerably stronger than a p-d coupling in π orbitals. The important question of whether the hole formation in the CuO_2 plane is restricted to $p\sigma$ orbitals or whether in-plane $p\pi$ orbitals are included, we cannot finally decide. The measurements give experimental evidence of p-d orbital hybridization in the (a,b) plane favoring σ bonds for the hole localization.

As a conclusion of our experiments, we can say that it is not only in the CuO_2 plane where the oxygenlike holes possessing the lowest binding energy can be expected. Our experimental polarized O $K\alpha$ spectra indicate that the holes in the BaO plane are also quite likely in the case of $YBa_2Cu_3O_7$ compound. Furthermore, the possible holes in the Cu-O chain cannot be excluded, either.

In a recent paper by Kottman *et al.*,[25] the polarized O $K\alpha$ spectra are presented. For c parallel to **e**, the feature at 527 eV was also observed.

[1] P. Steiner, V. Kinsinger, I. Sander, B. Siegwart, S. Hüfner, and C. Politis, Z. Phys. B **67**, 19 (1987).

[2] F. Werfel, M. Heinonen, and E. Suoninen, Z. Phys. B **70**, 317 (1988).

[3] P. Steiner, S. Hüfner, A. J. Jungmann, V. Kinsinger, and I. Sander, Z. Phys. B **74**, 173 (1988).

[4] J. H. Weaver, H. M. Meyer, III, T. J. Wagener, D. M. Hill, Y. Gao, D. Peterson, Z. Fisk, and A. J. Arko, Phys. Rev. B **38**, 4668 (1988).

[5] G. Dräger, F. Werfel, and J. A. Leiro, Phys. Rev. B **41**, 4050 (1990).

[6] G. van der Laan, C. Westra, C. Haas, and G. A. Sawatzky, Phys. Rev. B **23**, 4369 (1981).

[7] J. Zaanen, C. Westra, and G. A. Sawatzky, Phys. Rev. B **23**, 8060 (1986).

[8] D. E. Ramaker, Phys. Rev. B **38**, 11 816 (1988); D. E. Ramaker, N. H. Turner, and F. L. Hutson, *ibid.* **38**, 11 368 (1988).

[9] A. Fujimori, E. Takayama-Muromachi, and Y. Uchida, Solid State Commun. **63**, 857 (1987).

[10] N. Nücker, H. Romberg, X. X. Xi, J. Fink, B. Gegenheimer, and Z. X. Zhao, Phys. Rev. B **39**, 6619 (1989).

[11] J. Guo, D. E. Ellis, E. E. Alp, and G. L. Goodman, Phys. Rev. B **42**, 251 (1990).

[12] J. Zaanen, M. Alouani, and O. Jepsen, Phys. Rev. B **40**, 837 (1989).

[13] A. Bianconi, M. De Santis, A. Di Cicco, A. M. Flank, A. Fontaine, P. Legarde, H. Katayama-Yoshida, A. Kotani, and A. Marcelli, Phys. Rev. B **38**, 7196 (1988).

[14] D. W. Fisher, J. Appl. Phys. **36**, 2048 (1965); J. Chem. Phys. **42**, 3814 (1965).

[15] M. O. Krause and J. H. Oliver, J. Phys. Chem. Ref. Data **8**, 329 (1979).

[16] E. J. McGuire, Phys. Rev. A **2**, 273 (1970); **3**, 578 (1971).

[17] G. Dräger and O. Brümmer, Phys. Status Solidi B **124**, 11 (1984).

[18] P. Rennert, H. Schelle, and U.-H. Gläser, Phys. Status Solidi B **121**, 673 (1984).

[19] J. A. Leiro, F. Werfel, and G. Dräger, Phys. Rev. B **44**, 7718 (1991).

[20] A. Fujimori, Phys. Rev. B **39**, 793 (1989).

[21] J.-M. Mariot, V. Barnole, C. F. Hague, G. Vetter, and F. Queyroux, Z. Phys. B **75**, 1 (1989).

[22] J. A. Leiro, Philos. Mag. Lett. **57**, 189 (1988).

[23] H. Krakauer and W. Pickett, Phys. Rev. Lett. **60**, 1665 (1988).

[24] A. Kotani, *Conference Proceedings of the 2nd European Conference on Progress in X-Ray Synchrotron Radiation Research,* edited by A. Balerna, E. Bernieri, and S. Mobilio (SIF, Bologna, 1990), Vol. 25.

[25] A. Kottmann, F. Burgäzy, D. J. Lam, Y. Fang, P. Lamparter, and S. Steeb, Physica C **178**, 125 (1991).